Identification of Functionally Important Residues in the Pyridoxal-5′-Phosphate-Dependent Catalytic Antibody 15A9

Barbara Mouratou*,#,‡ and Jörg Stetefeld§

Biochemisches Institut der Universität Zürich, Winterthurerstrasse 190, CH-8057 Zürich, Switzerland, and Department of Biophysical Chemistry, Biozentrum, University of Basel, Klingelbergstrasse 70, CH-4056 Basel, Switzerland

Received January 15, 2004; Revised Manuscript Received March 14, 2004

ABSTRACT: Antibody 15A9 is unique in its ability to catalyze the transamination reaction of hydrophobic D-amino acids with pyridoxal-5′-phosphate (PLP). Both previous chemical modification studies and a three dimensional (3-D) homology model indicated the presence of functionally important tyrosine residues in the antigen-binding cavity of antibody 15A9. To gain further insight into the hapten, ligand binding, and catalytic mechanism of 15A9, all tyrosine residues in the complementarity-determining regions (CDRs) and the single arginine residue in CDR3 of the light chain were subject to an alanine scan. Substitution of Tyr(H33), Tyr(L94), or Arg(L91) abolished the catalytic activity and reduced the affinity for PLP and N^{α}-(5′-phosphopyridoxyl)-amino acids, which are close analogues of covalent PLP-substrate adducts. The Tyr(H100b)Ala mutant possessed no detectable catalytic activity, while its affinity for each ligand was essentially the same as that of the wild-type antibody. The binding affinity for the hapten was drastically reduced by a Tyr(L32)Ala mutation, suggesting that the hydroxyphenyl group of Tyr(L32) participates in the binding of the extended side chain of the hapten. The other Tyr → Ala substitutions affected both binding and catalytic activity only to a minor degree. On the basis of the information obtained from the mutagenesis study, we docked N^{α}-(5′-phosphopyridoxyl)-D-alanine into the antigen-binding site. According to this model, Arg(L91) binds the α-carboxylate group of the amino acid substrate and Tyr(H100b) plays an essential role in the catalytic mechanism of antibody 15A9 by facilitating the Cα/C4′ prototropic shift. In addition, the catalytic apparatus of antibody 15A9 revealed several mechanistic features that overlap with those of PLP-dependent enzymes.

More than one hundred antibodies that catalyze a wide variety of reactions, including many that cannot be achieved by standard chemical methods, have been generated to date (*1*). Although rate accelerations of 10^6-fold over uncatalyzed reactions and in a few cases rates approaching those of the corresponding enzyme-catalyzed reaction have been achieved (*2*−*4*), catalytic antibodies in general have not yet reached the rate enhancements characteristic of enzymes. However, it should be noted that many pathways and ideas still remain to be explored such as metal- or cofactor-containing antibodies or the evolution of catalytic antibodies under metabolically driven pressure (*5*).

The incorporation of nonproteinaceous cofactors into the binding sites of antibodies seems to be of interest, as it may extend the catalytic potential of antibodies. Pyridoxal-5′-phosphate (PLP),[1] a derivative of vitamin B_6, is probably the most versatile organic cofactor of enzymes and thus an attractive candidate for the generation of cofactor−dependent abzymes (*6*). The generation of the first monoclonal antibodies with PLP-dependent catalytic activity has been previously described (*7*, *8*). Immunization with the hapten N^{α}-(5′-phosphopyridoxyl)-L-lysine **1** (Figure 1 shows the hapten in N^{ϵ}-acetylated form) conjugated to maleylated keyhole limpet hemocyanin yielded 24 hapten-binding antibodies. Among these, two were found to catalyze PLP-dependent reactions.

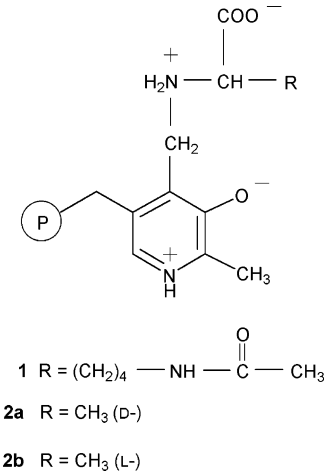

FIGURE 1: Structure of ligands used in binding studies: **1**, N^{α}-(5′-phosphopyridoxyl)-N^{ϵ}-acetyl-L-lysine; **2a**, N^{α}-(5′-phosphopyridoxyl)-D-alanine; **2b**, N^{α}-(5′-phosphopyridoxyl)-L-alanine.

* To whom correspondence should be addressed: E-mail: mouratou@lebs.cnrs-gif.fr; tel.: 33-1-69 82 35 00; Fax: 33-1-69 82 31 29.

Biochemisches Institut der Universität Zürich.

§ University of Basel.

‡ Present address: Laboratoire d'Enzymologie et de Biochimie Structurale, CNRS, 1 Avenue de la Terrasse, 91198 Gif sur Yvette Cedex, France.

[1] Abbreviations: CDR, complementarity-determining region; PLP, pyridoxal-5′-phosphate; PMP, pyridoxamine-5′-phosphate; PPL-, N^{α}-(5′-phosphopyridoxyl)-; V_H, variable region of the heavy chain; V_L, variable region of the light chain.

10.1021/bi049874e CCC: $27.50
Published on Web 05/07/2004

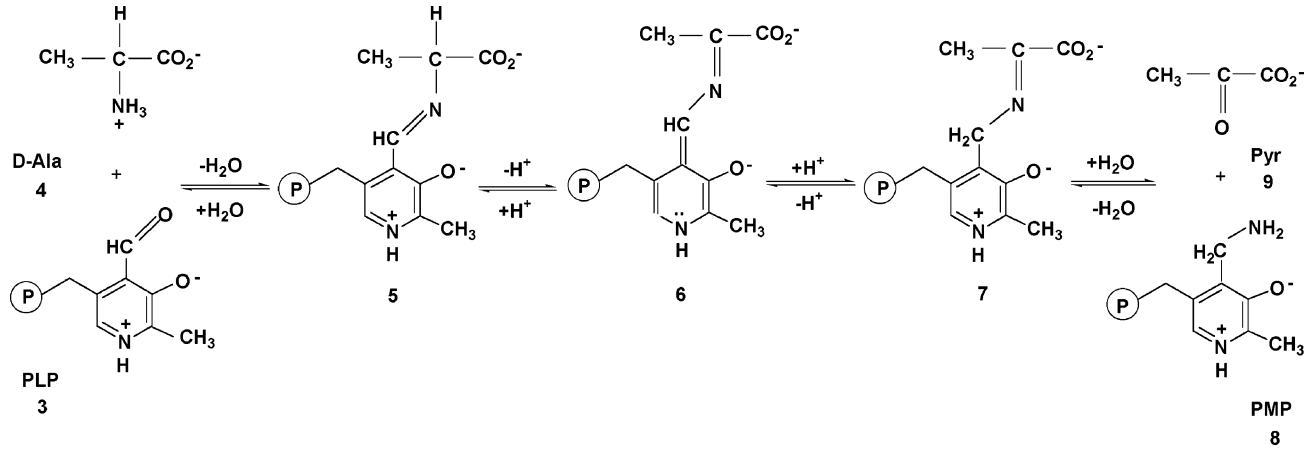

FIGURE 2: Transamination reaction of D-alanine and pyridoxal-5′-phosphate (PLP) as catalyzed by antibody 15A9. Catalysis of the reverse reaction has also been demonstrated (*7*).

Antibody 13B10 catalyzes the β-elimination reaction of β-chloro-L-alanine to chloride, ammonia, and pyruvate. Antibody 15A9 catalyzes the same reaction with the D-enantiomer of β-chloroalanine. In addition, it catalyzes full transamination reactions of hydrophobic D-amino acids and oxo acids with PLP and its aminated counterpart, pyridoxamine-5′-phosphate (PMP), respectively (e.g., $k_{cat} = 0.42$ min^{-1} with D-alanine and PLP at 25 °C; Figure 2). In comparison to the unassisted reactions of the PLP-amino acid aldimine **5**, the rate enhancement brought about by antibody 15A9 is 5×10^3 (*7*). The challenge, therefore, is to generate antibodies with increased efficiency starting from the first-generation antibody 15A9.

As a first step toward this goal, the amino acid sequence of the variable regions of the catalytic antibody 15A9 was determined by sequencing its cDNA (*9*). Consistent with a high tyrosine content in the complementarity-determining regions (CDRs), chemical modification of monoclonal antibody 15A9 by tetranitromethane has indicated that tyrosine residues are essential for both hapten binding and catalytic activity (*9*).

In the current study, we have mapped the active site of the catalytic antibody 15A9. To understand how the catalytic antibody 15A9 recognizes its substrate and accelerates the transamination reaction, we first constructed a 3-D model of the 15A9 Fv fragment by homology modeling. This model was used together with the chemical modification results as a guide for performing site-directed mutagenesis of the recombinant 15A9 Fab fragment. The data provided by this work allowed us to perform affinity docking of N^{α}-(5′-phosphopyridoxyl)-D-alanine (PPL-D-Ala), an analogue of the covalent PLP-substrate intermediate, in the three dimensional (3-D) model of the antibody. In conjunction with the site-directed mutagenesis experiments, these computational docking simulations served to identify the amino acid residues in antibody 15A9 that are critical for molecular recognition and catalysis.

EXPERIMENTAL PROCEDURES

Construction of Expression Plasmid and Mutagenesis. The Fab expression vector was constructed using the previously amplified polymerase chain reaction products of the variable regions of the heavy and light chains (V_H and V_L, respectively) of antibody 15A9 (*9*). The amplification products were purified by agarose gel electrophoresis and cut with the restriction enzymes PstI and BstEII in the case of V_H and SacI and XhoI in the case of V_L. The V_H and V_L genes were then separately inserted into the Fab expression vector pASK85 (*10*) that had been cut with the same enzymes, yielding pASK85−15A9. The mutants were prepared by polymerase chain reaction from pASK85−15A9 using the QuikChange Site-directed mutagenesis kit from Stratagene and the following primer pairs: Y-H32-Aa, 5′-GGGTTCAC-CTTCACTGAT*GC*CTACATGAGCTGGGTC-3′; Y-H32-Ab, 5′-GACCCAGCTCATGTAG*GC*ATCAGTGAAGGT-GAACCC-3′; Y-H33-Aa, 5′-CACCT-TCACTGATTAC*GC*-CATGAGCTGGGTCCGACAG-3′; Y-H33-Ab, 5′-CTGT-CGGACCC-AGCTCATG*GC*GTAATCAGTGAAGGT-G-3′; Y-H55-Aa, 5′-GGTCTTATTAGAAACAA-AGCTAAT-GGT*GC*CACAAAAGAGTACAGTGC-3′; Y-H55-Ab, 5′-GC-ACTGTACTCTT-TTGTG*GC*ACCATTAGCTTTGTTTCT-AATAAGACC-3′; Y-H59-Aa, 5′-GGTTACACAA-AAGAG-*GC*CAGTGCATCTGTGAAGGG-3′; Y-H59-Ab, 5′-CCCT-TCACAGATGCACTG-*GC*CTCTTTTGTGTAACC-3′; Y-H-99-Aa, 5′-GTAAGAGATAAGGGCTCG*GC*TGGTAA-CTA-CGAGGCCTGG-3′; Y-H99-Ab, 5′-CCAGGCCTCGTAGT-TACCA*GC*CGAGCC-CTTATCTCTTAC-3′; Y-H100b-Aa, 5′-GGGCTCGTATGGTAAC*GC*CGAGGCCTGGTT-TGCT-3′; Y-H100b-Ab, 5′-AGCAAACCAGGCCTCG*GC*GTTAC-CATACGAGCCC-3′; Y-L32-Aa, 5′-GCCACCTCAGGTG-TAAAT*GC*CATGCACTGGTTCCAGC-3′; Y-L32-Ab, 5′-G-CTGGAACCAGTGCATG*GC*ATTTACACCTGAGGTGG-C-3′; R-L91-Aa, 5′-GCCA-CTTATTACTGCCAGCAA*GC*-GAGTACTTACCCATTCACG-3′; R-L91-Ab, 5′-CGTGA-A-TGGGTAAGTACTC*GC*TTGCTGGCAGTAATAAGTGGC-3′; Y-L94-Aa, 5′-GCCAGC-AAAGGAGTACT*GC*CCCAT-TCACGTTCGGTGG-3′; and Y-L94-Ab, 5′-CCACCGAACG-TGAATGGG*GC*AGTACTCCTTTGCTGGC-3′. The mutations were verified by cycle sequencing (SequiTherm EXCEL II Long-Read DNA Sequencing Kit-LC, Epicentre Technologies) with fluorescent primers using a DNA sequencer (LI-COR).

Expression and Purification of Fab Fragments. Escherichia coli JM83 cells were used as hosts for pASK85-15A9 and the mutant plasmids. Cells transformed with the corresponding plasmid were grown in LB medium (50 mL) overnight at 37 °C in the presence of 100 μg/mL ampicillin. One liter of 2xYT medium in a 5-L shaking flask was

inoculated with 20 mL of the overnight culture and incubated at 37 °C until an A_{550} of 0.8 was reached. Expression was then induced by the addition of 100 μL of a 2 mg/mL solution of anhydrotetracycline (ACROS Chimica) in dimethylformamide. After further shaking of the sample for 4 h at 25 °C, the cells were harvested by centrifugation at 5000 rpm for 15 min. The Fab fragments were purified from the periplasmic cell extract by Immobilized Metal-Affinity chromatography as described previously (*11*). The purified Fab fragments were dialyzed extensively against 50 mM Bis-Tris propane, 140 mM NaCl, pH 7.5, and kept in the same buffer at 4 °C at a concentration of 0.7−1.0 mg/mL. All preparations were pure by the criterion of SDS−polyacrylamide gel electrophoresis. The concentration of purified Fab fragments was determined photometrically with a calculated absorption coefficient at 280 nm of 1.8 mL mg^{-1} cm^{-1}.

Measurement of Dissociation Equilibrium Constants. The synthesis of the haptens has been described previously (*7*, *8*). The thermodynamic binding affinities (K_d values) of wild-type and mutant Fab 15A9 for ligands were determined by the quenching of the intrinsic antibody fluorescence at 342 nm. The excitation wavelength was set to 280 nm (band-pass 0.45 nm), and emission was recorded from 290 to 430 nm (band-pass 4.50 nm) on a Spex Fluorolog spectrofluorimeter. Increasing concentrations of ligands were added to the Fab fragment (0.01−0.4 μM) in 50 mM Bis-Tris propane, 140 mM NaCl, pH 7.5 at 25 °C. After each addition, the fluorescence spectrum was recorded when equilibrium had been reached. All measurements were corrected for the fluorescence of the ligand itself. K_d values were calculated by nonlinear regression analysis.

Measurement of Transaminase Activity. The transaminase activity of the recombinant wild-type and mutant Fab fragments was measured by following the increase in absorbance at 325 nm ($\epsilon = 8300$ M^{-1} cm^{-1}; *12*) due to the production of PMP **8** (Figure 2). PLP **3** (200 μM) and D-alanine **4** (25−200 mM) were preincubated for 30 min in 50 mM Bis-Tris propane, 140 mM NaCl, pH 7.5, at 25 °C. The amount of the PLP-D-alanine Schiff base adduct **5**, which served as substrate for the transamination reaction, was calculated with the experimentally determined extinction coefficient $\epsilon_{410} = 3.7$ mM^{-1} cm^{-1} (*13*). The reaction was then started with the addition of 1−10 μM Fab 15A9. Controls without antibody were measured under identical conditions.

Molecular Modeling and Affinity Docking of PPL-D-Ala. A homology model of the 15A9 Fv fragment was built using the Homology module of the Insight II program package version 97 (MSI/Biosym, San Diego). For the V_L domain, the structure of the murine anti-rhinovirus Fab 17-1a (PDB code 1FOR, 2.75 Å resolution, 93% sequence identity, 95% similarity) was used as a template (*14*). The V_H domain was modeled using the anti-Brucella A cell wall polysaccharide Fab YST 9.1 (PDB code 1MAM, 2.45 Å resolution, 93% sequence identity, 95% similarity excluding CDR H3) as a template (*15*). The CDR H3 conformation was based on that of murine Fab HC19 (PDB code 1GIG, 2.3 Å resolution; *16*). Since the two templates used for the V_L and V_H domains differed in the relative orientation of the two domains, an intermediate relative domain orientation was chosen for the model. The model was submitted to 500 cycles of conjugate gradient minimization using the cvff force field and a distance-dependent dielectric in the Discover module of Insight II.

The substrate analogue PPL-D-Ala was docked to the 15A9 model using the program package FTDOCK (*17*). Manual adjustments of torsion angles and positional refinements were then performed. The atomic model of the antibody 15A9 with the substrate analogue PPL-D-Ala was energy-minimized with the program CNS (*18*). The coordinates of PPL-D-Ala in D-amino acid aminotransferase were used as a template (*19*). The refinement protocol has been performed applying constraints on the planar coenzyme−substrate adduct. Harmonic restraints were imposed on the protein atoms (3 kcal/mol/Å^2) with increased weight (20 kcal/mol/Å^2) for the Cα atoms.

RESULTS

Production of Recombinant Wild-Type and Mutant Fab 15A9. The expression of catalytic antibody 15A9 in a bacterial host was a prerequisite for this work because it allowed the functional consequences of specific mutations to be assessed. Recombinant antibody 15A9 was produced in *E. coli* as chimeric Fab with the murine variable regions being fused to murine constant regions of subclasses C_κ and $C_H1_\gamma1$ (*20*). The expression levels of wild-type protein were found to be similar to those of a variety of other antibodies expressed in the same way (200−250 μg/L; *11*). The binding affinities of the recombinant 15A9 Fab fragment for PLP and various N^α-5′-phosphopyridoxyl (PPL) amino acids (Figure 1) as determined by fluorescence titration and the catalytic activities were almost identical with those of the intact murine antibody(Figure 3, Tables 1 and 2). The mutant Fab fragments were isolated and purified by the same procedure and in similar yields as wild-type Fab (for details, see Experimental Procedures).

Choice of Mutants. The amino acid sequences of the PLP-dependent catalytic antibodies 15A9 and 13B10 and of five hapten-binding but noncatalytic antibodies have been determined previously by cDNA sequencing. Despite the independent origins of this panel of antibodies, they all seem to possess tyrosine residues essential for both hapten binding and catalytic activity as determined by chemical modification studies (*9*). Consequently, it would be expected that comparison with structurally related noncatalytic antibodies might be important in understanding the mechanism of action of antibody 15A9. However, antibody 15A9 did not show a high degree of amino acid sequence identity in both the V_H and V_L domain with any of the noncatalytic antibodies. Therefore, mutagenesis studies were necessary to identify the tyrosine residues important for binding and catalysis in antibody 15A9.

The 3-D structure of various immunoglobulins has been examined mainly by X-ray crystallography, and sufficient data are now available (*21*) to allow reliable computational 3-D modeling of antibody 15A9 (Figure 4). Antibody 15A9 possesses seven tyrosine residues in the CDRs of the heavy chain (H32, H33, H55, H59, H99, H100b, and H102) and two tyrosine residues (L32 and L94) in the CDRs of the light chain (Figure 5). Four of these tyrosine residues (L32, L94, H33, and H100b) reach into the area of space usually occupied by hapten antigens and are therefore potential candidates for contact residues. Tyrosine residues H32, H55,

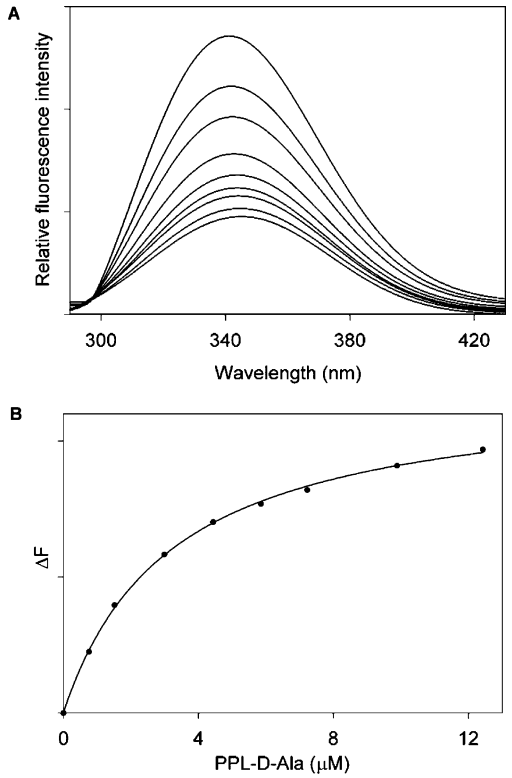

FIGURE 3: Fluorescence titration of wild-type Fab 15A9 with N^{α}-(5′-phosphopyridoxyl)-D-alanine (PPL-D-Ala **2a** in Figure 1). The measurements were performed in 50 mM Bis-Tris propane, 140 mM NaCl, pH 7.5, at 25 °C. (A) The ligand was added in a final concentration of 0.8−12 μM and quenched the intrinsic fluorescence of the antibody (0.28 μM). (B) The differences between the relative fluorescence intensity at 342 nm of Fab 15A9 alone and complexed with PPL-D-Ala, are plotted as a function of ligand concentration. For details, see Experimental Procedures.

Table 1: Dissociation Equilibrium Constants of Mutant and Wild-Type 15A9 Fab for PLP and N^{α}-5′-Phosphopyridoxyl (PPL) Amino Acids[a]

	K_d (μM)			
antibody	PPL-N^{ϵ}-acetyl-L-lysine	PLP	PPL-L-Ala	PPL-D-Ala
IgG 15A9[b]	0.03	90	1.5	1.5
Fab wild-type	0.02	110	2.1	3.2
Tyr(H32)Ala	0.06	178	28	13
Tyr(H33)Ala	0.40	360	48	50
Tyr(H55)Ala	0.02	132	4.4	6.5
Tyr(H59)Ala	0.03	90	2.3	3.5
Tyr(H99)Ala	0.02	135	3.4	4.0
Tyr(H100b)Ala	0.05	152	4.6	4.9
Tyr(L32)Ala	0.18	97	6.8	9.2
Tyr(L94)Ala	0.29	332	129	209
Arg(L91)Ala	0.20	295	199	312

[a] The constants were determined by measurement of the quenching of the intrinsic antibody fluorescence at 342 nm upon ligand addition at pH 7.5, and 25 °C. For details, see Figure 3 and Experimental Procedures. The errors on determination of K_d are less than ± 8%. [b] The values are taken from ref *7*.

H59, and H99 point away from the putative antigen-binding pocket (Figure 4), they are located, however, in positions where a substitution by alanine might influence CDR conformation and thus indirectly affect antigen binding and catalysis. Thus, all the above tyrosine residues were mutated to alanine by site-directed mutagenesis. Tyr(H102), which faces away from the binding pocket (*22*) and is located in a position with low backbone conformation variability because it is embedded in the β-sheet, was not mutated. One of the arginine residues in the binding pocket (L91), which is the only arginine residue in CDR L3 of antibody 15A9 (Figure 5), was also substituted by alanine, as the important contribution of arginine residues to antibody affinity and catalysis toward anionic ligands has been emphasized previously (*23*, *24*) and holds also true for enzymes (*25*).

Table 2: Kinetic Constants for the Transamination Half-Reaction Catalyzed by Wild-Type and Mutant 15A9 Fab[a]

antibody	k_{cat} (min^{-1})	K_m (μM)	k_{cat}/K_m (min^{-1} M^{-1})
IgG 15A9[b]	0.42	65	6.5×10^3
Fab wild-type	0.40	76	5.4×10^3
Tyr(H32)Ala	0.08	121	0.7×10^3
Tyr(H33)Ala	b.d.[c]		
Tyr(H55)Ala	0.19	101	1.8×10^3
Tyr(H59)Ala	0.39	108	3.6×10^3
Tyr(H99)Ala	0.40	106	3.8×10^3
Tyr(H100b)Ala	b.d.[c]		
Tyr(L32)Ala	0.19	118	1.6×10^3
Tyr(L94)Ala	0.020[d]		
Arg(L91)Ala	0.027[d]		

[a] The k_{cat} and K_m values were determined at pH 7.5 and 25 °C as described under Experimental Procedures. The K_m values are for the PLP-D-alanine Schiff base adduct. The rates of the antibody-catalyzed reactions were corrected for the rates of the corresponding uncatalyzed reactions measured in the same buffer system without added antibody. The errors on kinetic parameters are ± 15%. [b] From ref *7*. [c] b.d., below detection. [d] Rates measured at 200 μM PLP and 200 mM D-alanine without reaching saturation.

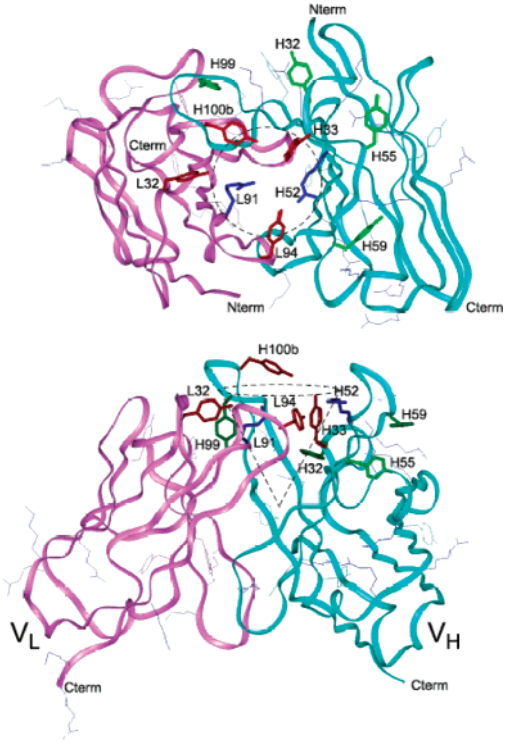

FIGURE 4: Homology model of the 15A9 Fv fragment. Dashed lines outline the binding pocket utilized by the majority of the hapten-binding antibodies. Tyrosine and basic residues in the vicinity of the binding pocket have been highlighted: Tyrosine residues L32, L94, H33, and H100b (red) and Arg L91 and H52 (blue) were predicted to have a high probability of making direct antigen contact, while TyrH32, H55, H59, and H99 (green) were predicted to have a low probability of making direct contact but to potentially have an indirect effect on antigen binding.

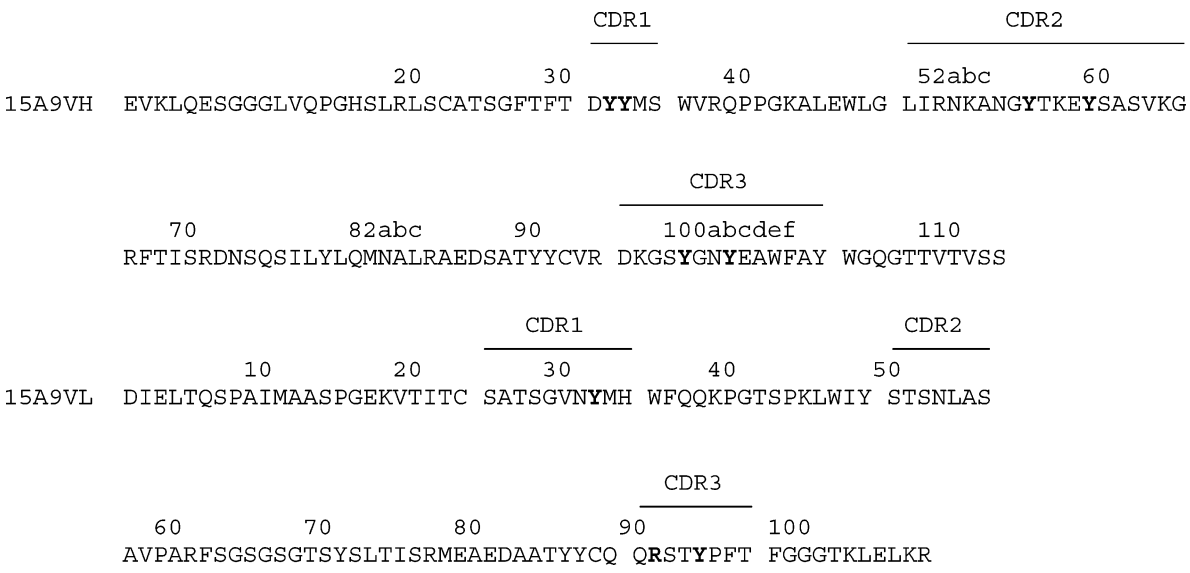

FIGURE 5: Primary structure of heavy and light chain variable regions (V_H and V_L) of antibody 15A9 (*9*). Numbering of amino acid residues and CDR designation are according to Kabat et al. (*20*). The residues that were mutated in this study are indicated in bold.

Binding and Catalytic Activities of Mutant Fabs 15A9. The dissociation equilibrium constants for the hapten, PLP, and PPL-alanine (Table 1) as well as the PLP-dependent transaminase activity toward D-alanine (Table 2) were determined for each mutant. The preserved affinity of an antibody mutant for its hapten **1** (Figure 1) provides the most direct indication that a nativelike structure has been retained. The K_d values for PLP and of the covalent coenzyme−substrate adduct analogues PPL-D-Ala **2a** (Figure 3) and its enantiomer PPL-L-Ala **2b** were measured to differentiate between the consequences of the mutations on the binding of the coenzyme and the substrate moiety (Table 1).

As expected from our model, substitution of Tyr(H59) and Tyr(H99) by alanine changed neither the binding affinities nor the catalytic activities (Table 2). With this confidence in the model, we further examined the role of mutated residues. Replacement of Tyr(H55) and Tyr(L32) with alanine resulted in a 2-fold decrease in k_{cat}. The binding affinities of Fab 15A9 Tyr(H55)Ala for all ligands were similar to those of wild-type Fab 15A9 (Table 1). In contrast, the Tyr(L32)Ala mutation reduced the binding affinity for hapten **1** (Figure 1) 10-fold, while the binding affinities for PLP, PPL-D-Ala, and PPL-L-Ala were nearly the same as those of the wild-type Fab, suggesting that the hydroxyphenyl group of Tyr(L32) participates in the binding of the extended side chain of the hapten. The residual catalytic activity of the latter two mutants suggests that neither Tyr(H55) nor Tyr(L32) is essential for catalysis. The binding affinities of the Tyr(H32)Ala mutant for PLP and hapten were close to those of the wild-type Fab, suggesting that the active site had remained largely intact. However, the binding affinities for the substrate analogue PPL-D-Ala and its enantiomer PPL-L-Ala were reduced 5- and 15-fold, respectively. The catalytic activity of this mutant was decreased 5-fold. Tyr(H32) may thus assist catalysis by favorably orientating Tyr(H33), which in turn affects ligand binding and catalysis.

A dramatic change in catalytic activity was observed when Tyr(H100b) in the CDR H3 was replaced with alanine. Fab Tyr(H100b)Ala was devoid of detectable catalytic activity (Table 2). The binding affinity for the ligands was nearly the same as that of wild-type Fab (Table 1), suggesting that the reduced catalytic activity of the mutant was not due to a conformational disruption of the antibody active site. Obviously, Tyr(H100b) plays an essential role in the catalytic mechanism of antibody 15A9.

Substitution of Tyr(H33) abolished the catalytic activity. The parallel decrease in binding of coenzyme−amino acid adducts is consistent with the notion that Tyr(H33) participates in the positioning of PLP, which is common to all ligands. Substitution of this residue might destabilize the planar transition states of the aldimine−ketimine tautomerization in the transamination reaction (*36*) and thus result in the complete loss of catalytic activity.

Substitution of Tyr(L94) and Arg(L91) resulted in both impaired ligand binding and substantially reduced catalytic efficiency. The fact that the affinity of these mutants for hapten and PLP is not severely altered (an approximately 10- and 3-fold decrease, respectively) argues against drastic structural changes in the coenzyme-binding site. However, the significant decrease observed in both the binding affinities for PPL-D-Ala (65- and 98-fold decrease for the Tyr(L94)-Ala and Arg(L91)Ala mutant, respectively) and the substrate affinity indicate a substantial perturbation in the environment surrounding the amino acid substrate moiety.

Affinity Docking of PPL-D-Ala to the 15A9 Homology Model. Affinity docking experiments often predict that the hapten and/or the substrate have several possible binding modes (*26*). The selection among the possible docked structures requires additional experiments. Here, we docked the substrate analogue PPL-D-Ala in planar conformation into the antigen-binding pocket of the model, based on the results obtained from the site-directed mutagenesis (Figure 6).

The cofactor-binding region is located at the interface of the two domains and is mainly composed of residues of CDR H1, CDR H3, CDR L1, and CDR L3. The model suggests that the cofactor interacts with residues in the active site of 15A9 through numerous hydrogen bonding and hydrophobic packing interactions, such that the *si* face of the pyridine ring is solvent-exposed, and the *re* face oriented toward the protein. The pyridine ring of the cofactor is engaged in an aromatic stacking interaction with Tyr(H33). The positive charge of the protonated pyridine nitrogen atom is balanced

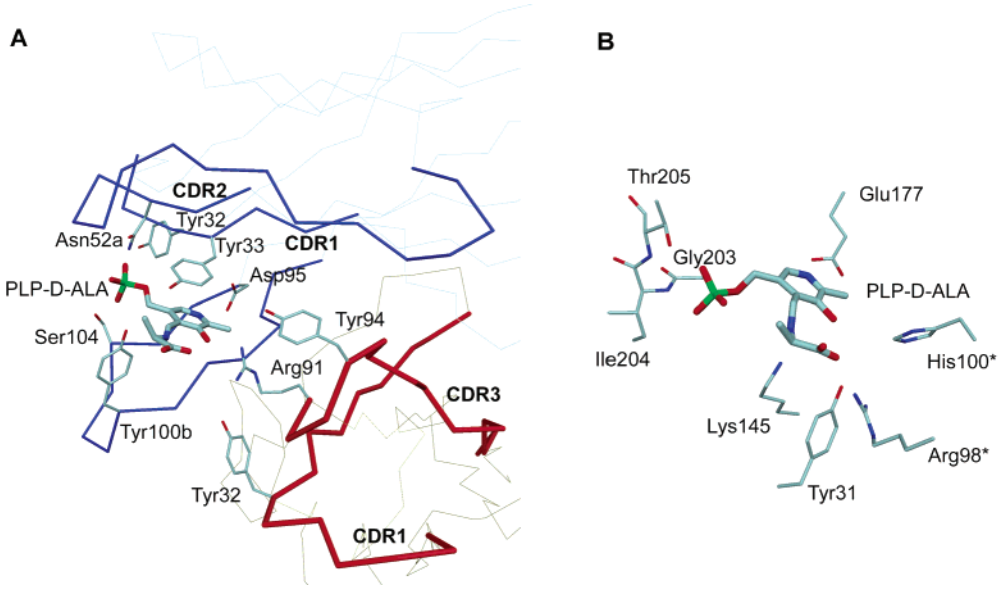

FIGURE 6: Comparison of the active sites of antibody 15A9 and D-amino acid aminotransferase. (A) Homology model of the Fv fragment of antibody 15A9 liganded with a planar covalent coenzyme-D-alanine adduct (PLP-D-ALA, corresponding to intermediates **5**−**7** in Figure 2). The heavy chain is drawn in light-blue with the CDRs in blue and bold. The light chain is colored in light red with the CDRs in red and bold. The coenzyme−substrate adduct is drawn in gray. Important side chains are numbered according to Kabat et al. (*20*). (B) Crystal structure of D-amino acid aminotransferase (D-alanine aminotransferase, EC 2.6.1.21). The coordinates are from Peisach et al. (PDB code 3DAA) (*19*). Amino acid residues contributed by the adjacent subunit are marked with an asterisk.

by a hydrogen bond to the carboxylate group of Asp(H95). The O3′ atom of the pyridine ring has no antibody ligand. The 5′-phosphate group of the cofactor is fixed via hydrogen bond interactions between the side chains of Tyr(H32), Asn(H52a), and Ser(H104) of CDR1, 2, and 3, respectively, of the heavy chain. In addition, the side chain of Tyr(H100b) is positioned close to the phosphate group of the cofactor forming a hydrogen bond between its phenolic hydroxyl group and the coenzyme phosphate. Noncovalent binding of PLP, which, in antibody 15A9, serves as a dissociable cofactor, is confirmed by the similar K_d values for PLP and PMP, i.e., 90 and 40 μM, respectively (*7*). Tyr(H32) has a structural role that appears to be the stabilization of the interaction between CDR H1 and CDR H2.

The model revealed that the guanidinium group of Arg(L91) lies at the bottom of the binding pocket, forming a salt bridge/hydrogen bond with the carboxylate group of the substrate. Arg(L91) together with Tyr(L32) and Tyr(L94) act as a carboxylate trap. These three residues together with the coenzyme seem to define the position and the orientation of substrate in the binding site of antibody 15A9. The positioning of the bound substrate relative to Tyr(H100b) appears to define the enantiomeric selectivity of the antibody. Only a D-amino acid would have its α-proton pointing toward the catalytic residue. The side chain of the substrate lies in a large pocket which accounts for the accommodation of a wide range of D-amino acid substrates (*7*).

DISCUSSION

Previous studies have shown that antibodies, which are selected in vivo for binding of a transition-state analogue and screened ex vivo for catalytic activity, may recapitulate a number of characteristics of enzymes, the evolution of which has been directed toward increased catalytic efficiency; examples of such congruent features include the molecular interactions underlying substrate recognition, stabilization of transition states, and principal mechanistic determinants (*27*, *28*). Despite the great number of catalytic antibodies that have been generated to date, only a few investigations on the structural requirements for catalysis and comparisons of the antibody-catalyzed and the corresponding enzyme-catalyzed reactions have been reported (*4*, *27*). Site-directed mutagenesis and computer-assisted construction of structural models of catalytic antibodies can provide insight into the contributions of individual amino acid residues to both binding and catalysis (*29*−*32*). Here, we undertook an alanine scanning and structural modeling study of the catalytic antibody 15A9, which may be considered an analogue of primordial PLP-dependent enzymes (*33*, *34*).

The candidate amino acid residues for site-directed mutagenesis studies were selected on the basis of previous chemical modification studies of the antibody (*9*), the homology model, and the knowledge on the catalytic mechanism of PLP-dependent enzymes (B_6 enzymes) (*33*, *35*, *36*). In PLP-dependent enzymes, tyrosine and arginine residues have been found to partake in coenzyme binding, substrate recognition, as well as in the catalytic process (*33*, *35*, *37*, *38*). In antibodies, the disproportionate number of tyrosine residues in CDRs and especially in the CDRs of the heavy chain has been emphasized in several previous reports (*22*, *39*). It has been pointed out that the hydroxyphenyl group of tyrosine may participate in both polar and apolar interactions. Chemical modification of antibody 15A9 with tetranitromethane has indeed indicated the participation of tyrosine residues in both hapten binding and catalytic activity (*9*). The positively charged side chain of arginine residues of CDR L3 has been found to allow binding and polarization of anionic substrates for nucleophilic attack and stabilization of anionic tetrahedral transition states by electrostatic interactions in catalytic antibodies (*23*, *40*, *41*).

As we have previously reported, antibody 15A9 catalyzes the transamination reaction of D-alanine with PLP through

the mechanism shown in Figure 2 (*7*, *8*). Schiff base **5** (formed from PLP **3** and D-alanine **4**) is, under the conditions used in this study (see Experimental Procedures), the actual substrate for the antibody. Deprotonation at Cα leads to the quinonoid intermediate **6**. Reprotonation at C4′ of the coenzyme moiety and hydrolysis of the ensuing ketimine intermediate **7** complete the transamination half reaction producing pyruvate **8** and PMP **9**. Catalytic activity is observed exclusively with the D-enantiomer of alanine. Antibody 15A9 in the presence of PLP catalyzes the exchange of the pro-2S proton of [2-^{13}C] glycine about 6 times faster than that of the pro-2R proton (*42*). The preferential deprotonation of the pro-2S proton of glycine agrees with the exclusive transamination of D-amino acids, as exchange of the pro-2S proton of glycine corresponds to the deprotonation at Cα of D-amino acids.

Substitution of Tyr(H100b) with alanine abolishes the catalytic activity with little effect on ligand binding. Tyr(H100b) clearly plays a role in catalysis, even though the precise details of this role are uncertain depending on the protonation state of the phenolic hydroxyl group. A mechanism involving nucleophilic attack by water or hydroxide ions assisted by hydrogen bonding provided by the undissociated form of the tyrosine side chain is a formal possibility. Alternatively, neighboring residues can activate the hydroxyl group of Tyr(H100b) for direct nucleophilic attack. Indeed, docking experiments suggest a plausible orientation of the substrate in which the Cα proton is close to the phenolic hydroxyl group of Tyr(H100b). Such mechanisms involving nucleophilic catalysis by a binding-site residue have been found in several catalytic antibodies (*2*, *43*). While the model of antibody 15A9 (Figure 6) suggests that Tyr(H100b) plays a role in the deprotonation at Cα, it shows no evident general acid group appropriately positioned for assisting the reprotonation at C4′. Possibly, Tyr(H100b) functions as a single catalytic residue that both abstracts a proton from Cα and then delivers a proton to C4′. In enzymatic transamination, the PLP-binding lysine residue serves such a double role (*44*), and even though there are relatively few examples of tyrosine functioning as a general acid in enzymatic reactions (e.g., in the PLP-dependent enzyme tyrosine phenol-lyase), Tyr71 has been proposed to fulfill this function (*45*).

After affinity docking with PPL-D-Ala, we compared the modeled structure of antibody 15A9 with the active site structure of PLP-dependent enzymes, aminotransferases in particular. This analysis revealed a number of convergent features underlying substrate recognition: (i) In the model, Arg(L91) seem to bind, together with Tyr(L32) and Tyr(L94), the α-carboxylate group of the amino acid substrate. A similar mode of binding is evident in the crystal structure of D-amino acid aminotransferase (Figure 6), where the carboxylate group of the substrate engages in interactions with Arg98, His100, and Tyr31 (*19*). Arginine is the preferred residue not only for binding amino acid substrates to PLP-dependent enzymes but also for binding carboxylic substrates to enzymes in general. The resonance-stabilized ion pair underlying the two hydrogen bonds that can be formed results in a peculiarly strong interaction of well-defined geometry (*45*, *46*). (ii) Tyr(H33) and Asp(H95) seem to interact with the pyridine ring of the coenzyme of the catalytic antibody in much the same way as tyrosine and aspartate residues engage in aromatic and electrostatic interactions with the PLP ring and with the positively charged pyridine nitrogen atom, respectively, in many B_6 enzymes (*33*, *35*, *44*−*48*).

The mutational analysis of 15A9 has provided valuable predictions regarding substrate binding and catalysis of the PLP-dependent transamination reaction. In particular, the data presented here indicate that tyrosine and arginine residues in the catalytic antibody 15A9 play roles similar to those fulfilled by such residues in B_6 enzymes. These results may be expected to prove useful in guiding the design of more effective catalysts that certainly would require substitutions of numerous amino acid residues that do not participate in the active site and thus the construction and screening of large libraries of random variants. Work in this direction is in progress.

ACKNOWLEDGMENT

We are grateful to A. Skerra for providing us with the Fab expression vector pASK85. We would also like to thank P. Christen and A. Honegger for useful discussions, and A.H. for help with Figure 4.

REFERENCES

1. Hilvert, D. (2000) Critical analysis of antibody catalysis, *Annu. Rev. Biochem. 69*, 751−793.
2. Wirsching, P., Ashley, J. A., Benkovic, S. J., and Lerner, R. A. (1991) An unexpectedly efficient catalytic antibody operating by ping-pong and induced fit mechanisms, *Science 252*, 680−685.
3. Jacobsen, J. R., Prudent, J. R., Kochersperger, L., Yonkovich, S., and Schultz, P. G. (1992) An efficient antibody-catalyzed aminoacylation reaction, *Science 256*, 365−367.
4. Barbas, C. F., Heine, A., Zhong, G., Hoffmann, T., Gramatikova, S., Bjornestedt, R., List, B., Anderson, J., Stura, E. A., and Wilson, I. A. (1997) Immune versus natural selection: antibody aldolases with enzymic rates but broader scope, *Science 278*, 2085−2092.
5. Green, B. S. (2002) Introduction, *J. Immunol. Methods 269*, 3−4.
6. Jencks, W. P. (1969) *Catalysis in Chemistry and Enzymology. Mechanisms for Catalysis*, p 133, McGraw-Hill, New York.
7. Gramatikova, S. I., and Christen, P. (1996) Pyridoxal 5′-phosphate-dependent catalytic antibody, *J. Biol. Chem. 271*, 30583−30586.
8. Gramatikova, S. I., and Christen, P. (1997) Monoclonal antibodies against N^{α}-(5′-phosphopyridoxyl)-L-lysine, *J. Biol. Chem. 272*, 9779−9784.
9. Mouratou, B., Gramatikova, S. I., Kunz, B., and Christen, P. (2000) Amino acid sequences and hapten binding of catalytic and noncatalytic antibodies against N^{α}-(5′-phosphopyridoxyl)-L-lysine, *Mol. Immunol. 37*, 633−640.
10. Skerra, A. (1994) Use of the tetracycline promoter for the tightly regulated production of a murine antibody fragment in *Escherichia coli*, *Gene 151*, 131−135.
11. Skerra, A. (1994) A general vector, pASK84, for cloning, bacterial production, and single-step purification of antibody Fab fragments, *Gene 141*, 79−84.
12. Peterson, E. A., and Sober, H. A. (1954) Preparation of crystalline phosphorylated derivatives of vitamin B_6, *J. Am. Chem. Soc. 76*, 169−175.
13. Matsuo, Y. (1957) Formation of Schiff bases of pyridoxal phosphate. Reaction with metal ions, *J. Am. Chem. Soc. 79*, 2011−2015.
14. Liu, H., Smith, T. J., Lee, W. M., Mosser, A. G., Rueckert, R. R., Olson, N. H., Cheng, R. H., and Baker, T. S. (1994) Structure determination of an Fab fragment that neutralizes human rhinovirus 14 and analysis of the Fab-virus complex, *J. Mol. Biol. 240*, 127−37.
15. Rose, D. R., Przybylska, M., To, R. J., Kayden, C. S., Oomen, R. P., Vorberg, E., Young, N. M., and Bundle, D. R. (1993) Crystal structure to 2.45 Å resolution of a monoclonal Fab specific for the Brucella A cell wall polysaccharide antigen, *Protein Sci. 2*, 1106−1113.

16. Bizebard, T., Daniels, R., Kahn, R., Golinelli Pimpaneau, B., Skehel, J. J., and Knossow, M. (1994) Refined 3-dimensional structure of the Fab fragment of a murine IGG1, lambda antibody, *Acta Crystallogr., Sect. D.: Biol. Crystallogr. 50*, 768−777.
17. Gabb, H. A., Jackson, R. M., and Sternberg, M. J. (1997) Modeling protein docking using shape complementarity, electrostatics and biochemical information, *J. Mol. Biol. 272*, 106−120.
18. Brünger, A. T., Adams, P. D., Clore, G. M., DeLano, W. L., Gros, P., Grosse-Kunstleve, R. W., Jiang, J. S., Kuszewski, J., Nilges, M., Pannu, N. S., Read, R. J., Rice, L. M., Simonson, T., and Warren, G. L. (1998) Crystallography & NMR system: A new software suite for macromolecular structure determination, *Acta Crystallogr., Sect. D: Biol. Crystallogr. 54*, 905−921.
19. Peisach, D., Chipman, D. M., Van Ophem, P. W., Manning, J. M., and Ringe, D. (1998) Crystallographic study of steps along the reaction pathway of D-amino acid aminotransferase, *Biochemistry 37*, 4958−4967.
20. Kabat, E. A., Wu, T. T., Perry, H. M., Gottesman, K., and Foeller, C. (1991) *Sequences of Proteins of Immunological Interest*, 5th ed., United States Department of Health and Human Services, National Institutes of Health, Bethesda, MD.
21. Bernstein, F. C., Koetzle, T. F., Williams, C. J. B., Meyer, E. F., Jr., Brice, M. D., Rodgers, J. R., Kennard, O., Shimanouchi, T., and Tasumi, M. (1997) The Protein Data Bank: a computer-based archival file for macromolecular structures, *J. Mol. Biol. 112*, 535−542.
22. Chothia C., and Lesk, A. M. (1987) Canonical structures for the hypervariable regions of immunoglobulins, *J. Mol. Biol. 196*, 901−917.
23. Mian, S., Bradwell, A. R., and Olson, A. I. (1991) Structure, function and properties of antibody binding sites, *J. Mol. Biol. 217*, 133−151.
24. Stewart, J. D., Roberts, V. A., Thomas, N. R., Getzoff, E. D., and Benkovic, S. J. (1994) Site-directed mutagenesis of a catalytic antibody: an arginine and a histidine residues play key roles, *Biochemistry 33*, 1994−2003.
25. Riordan, J. F., McElvany, K. D., and Borders, C. L., Jr. (1977) Arginyl residues: anion recognition sites in enzymes, *Science 195*, 884−886.
26. Hotta, K., Lange, H., Tantillo, D. J., Houk, K. N., Hilvert, D., and Wilson, I. A. (2000) Catalysis of decarboxylation by a preorganized heterogeneous microenvironment: crystal structures of abzyme 21D8, *J. Mol. Biol. 302*, 1213−1225.
27. Stewart, J. D., Krebs, J. F., Siuzdak, G., Berdis, A. J., Smithrud, D. B., and Benkovic, S. J. (1994) Dissection of an antibody-catalyzed reaction, *Proc. Natl. Acad. Sci. U.S.A. 91*, 7404−7409.
28. Kolesnikov A. V., Kozyr, A. V., Alexandrova, E. S., Koralewski, F., Demin, A. V., Titov, M. I., Avalle, B., Tramontano, A., Paul, S., Thomas, D., Gabibov, A. G., and Friboulet, A. (2000) Enzyme mimicry by the antiidiotypic antibody approach, *Proc. Natl. Acad. Sci. U.S.A. 97*, 13526−13531.
29. Gao Q.-S., Sun, M., Rees, A. R., and Paul, S. (1995) Site-directed mutagenesis of proteolytic antibody light chain, *J. Mol. Biol. 253*, 658−664.
30. Miyashita, H., Hara, T., Tanimura, R., Fukuyama, S., Cagnon, C., Kohara, A., and Fujii, I. (1997) Site-directed mutagenesis of active site contact residues in a hydrolytic abzyme: Evidence for an essential histidine involved in transition state stabilization, *J. Mol. Biol. 267*, 1247−1257.
31. Romesberg, F. E., Flanagan, M. E., Uno, T., and Schultz, P. G. (1998) Mechanistic studies of an antibody-catalyzed elimination, *J. Am. Chem. Soc. 120*, 5160−5167.
32. Hotta, K., Wilson, I. A., and Hilvert, D. (2002) Probing ligand recognition in the decarboxylase antibody 21D8: implications for the catalytic mechanism, *Biochemistry 41*, 772−779.
33. Mehta, P. K., and Christen, P. (2000) The molecular evolution of pyridoxal-5′-phosphate-dependent enzymes, *Adv. Enzymol. RAMB 74*, 129−184.
34. Christen, P., and Mehta, P. K. (2001) From cofactor to enzymes. The molecular evolution of pyridoxal-5′-phosphate-dependent enzymes, *The Chem. Rec. 1*, 436−447.
35. Jansonius, J. N. (1998) Structure, evolution and action of vitamin B_6-dependent enzymes, *Curr. Opin. Struct. Biol. 8*, 759−769.
36. Metzler, D. E. (2001) *Biochemistry*, 2nd ed., pp 737−753, Harcourt/Academic Press, New York.
37. Sundararaju, B., Antson, A. A., Phillips, R. S., Demidkina, T. V., Barbolina, M. V., Gollnick, P., Dobson, G. G., and Wilson, K. S. (1997) The crystal structure of *Citrobacter freundii* tyrosine phenol-lyase complexed with 3-(4′-hydroxyphenyl)propionic acid, together with site-directed mutagenesis and kinetic analysis, demonstrates that arginine 381 is required for substrate specificity, *Biochemistry 36*, 6502−6510.
38. Vacca, R. A., Giannattasio, S., Graber, R., Sandmeier, E., Marra, E., and Christen, P. (1997) Active-site Arg → Lys substitutions alter reaction and substrate specificity of aspartate aminotransferase, *J. Biol. Chem. 272*, 21932−21937.
39. Kabat, E. A., Wu, T. T., and Bilofsky, H. (1977) Unusual distribution of amino acids in complementarity-determining (hypervariable) segments of heavy and light chains of immunoglobulins and their possible roles in specificity of antibody-combining sites, *J. Biol. Chem. 252*, 6609−6616.
40. Patten, P. A., Gray, N. S., Yang, P. L., Marks, C. B., Wedemayer, G. J., Boniface, J. J., Stevens, R. C., and Schultz, P. G. (1996) The immunological evolution of catalysis, *Science 271*, 1086−1091.
41. Fujii, I., Fukuyama, S., Iwabuchi, Y., and Tanimura, R. (1998) Evolving catalytic antibodies in a phage-displayed combinatorial library, *Nat. Biotechnol. 16*, 463−467.
42. Mahon, M. M., Gramatikova, S. I., Christen, P., Fitzpatrick, T. B., and Malthouse, J. P. G. (1998) The pyridoxal-5′-phosphate-dependent catalytic antibody 15A9: Its efficiency and stereospecificity in catalysing the exchange of the α-protons of glycine, *FEBS Lett. 427*, 74−78.
43. Thayer, M. M., Olender, E. H., Arvai, A. S., Koike, C. K., Canestrelli, I. L., Stewart, J. D., Benkovic, S. J., Getzoff, E. D., and Roberts, V. A. (1999) Structural basis for amide hydrolysis catalyzed by the 43C9 antibody, *J. Mol. Biol. 291*, 329−345.
44. Kirsch, J. F., Eichele, G., Ford, G. C., Vincent, M. G., Jansonius, J. N., Gehring, H., and Christen, P. (1984) Mechanism of action of aspartate aminotransferase proposed on the basis of its spatial structure, *J. Mol. Biol. 174*, 497−525.
45. Chen, H., Demidkina, T. V., and Phillips, R. S. (1995) Site-directed mutagenesis of tyrosine 71 to phenylalanine in *Citrobacter freundii* tyrosine phenol-lyase: evidence for dual roles of tyrosine 71 as a general acid catalyst in the reaction mechanism and in the cofactor binding, *Biochemistry 34*, 12276−12283.
46. Hwang, J.-K., and Warshel, A. (1988) Why ion pair reversal by protein engineering is unlikely to succeed, *Nature 334*, 270−272.
47. Mitchell, J. B. O., Thornton, J. M., Singh, J., and Price, S. L. (1992) Towards an understanding of the arginine-aspartate interaction, *J. Mol. Biol. 226*, 251−262.
48. Antson, A. A., Demidkina, T. V., Gollnick, P., Dauter, Z., Von Tersch, R. L., Long, J., Berezhnoy, S. N., Phillips, R. S., Harutyunyan, E. H., and Wilson, K. S. (1993) Three-dimensional structure of tyrosine phenol-lyase, *Biochemistry 32*, 4195−4206.

BI049874E